JOC Article

Lanthanide Triflate-Catalyzed Arene Acylation. Relation to Classical Friedel–Crafts Acylation

Alma Dzudza and Tobin J. Marks*

Department of Chemistry, Northwestern University, 2145 Sheridan Road, Evanston, Illinois 60208-3113

t-marks@northwestern.edu

Received January 22, 2008

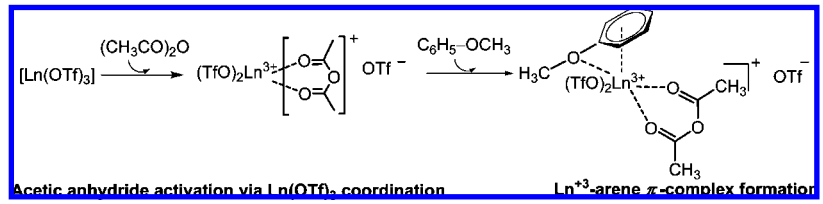

Lanthanide trifluoromethanesulfonates, $Ln(OTf)_3$ (OTf^- = trifluoromethanesulfonate), serve as effective precatalysts for the rapid, regioselective, intermolecular acylation of activated arenes. This contribution probes mechanism and metal ionic radius effects in the catalytic lanthanide triflate-mediated acylation of anisole with acetic anhydride. Kinetic studies of $Ln(OTf)_3$ (Ln = La, Eu, Yb, Lu)-mediated anisole acylation with acetic anhydride in nitromethane reveal the rate law $v \sim k_3\,[Ln^{3+}]^1[\text{acetic anhydride}]^1[\text{anisole}]^1$. Eyring and Arrhenius analyses yield $\Delta H^{\ddagger} = 12.9$ (4) kcal·mol^{-1}, $\Delta S^{\ddagger} = -44.8$ (1.3) e.u., and $E_a = 13.1$ (4) kcal·mol^{-1} for Ln = Yb, with the negative $\Delta S^{\ddagger}$ implying a highly organized transition state. The observed primary kinetic isotope effect of $k_H/k_D = 2.6 \pm 0.15$ is consistent with arene C−H bond scission in the turnover-limiting step. The proposed catalytic pathway involves precatalyst formation via interaction of $Ln(OTf)_3$ with acetic anhydride, followed by Ln^{3+}−anisole π-complexation, substrate−electrophile σ-complex formation, and turnover-limiting C−H bond scission. Lanthanide size effects on turnover frequencies are consistent with a transition state lacking significant ionic radius-dependent steric constraints. Substrate−Ln^{3+} interactions using paramagnetic Gd^{3+} and Yb^{3+} NMR probes and factors affecting reaction rates such as arene substituent and added $LiClO_4$ cocatalyst are also explored.

Introduction

The most important synthetic organic transformations are arguably those that generate carbon−carbon bonds, such as reactions which facilitate assembly of new molecular frameworks.[1] In this context, one of the most significant recent synthetic advances has been the development of broad classes of Lewis acid-catalyzed reactions, of great interest due to their unique reactivity and selectivity patterns.[1,2]

The Friedel–Crafts (FC) acylation of arenes is a fundamental and useful carbon−carbon bond-forming transformation for the preparation of aromatic ketones.[3] Classical intermolecular FC arene acylations are typically mediated by strong, moisture-sensitive Lewis acids such as $AlCl_3$, $TiCl_4$, and BF_3 in organic solvents.[3a,b,4] Acylations must be carried out under anhydrous conditions and require an acylating agent, e.g., an acyl chloride, acyl anhydride, or carboxylic acid, an aromatic substrate, and a stoichiometric excess of Lewis acid.[3a,b,4] Aluminum trichloride is often referred to as a "catalyst" even though it is known to be required in greater than stoichiometric amounts due to formation of stable Lewis acid−aryl ketone product complexes, thus necessitating a final hydrolysis step for product isolation.[3,4] This reaction is catalytic only if the Lewis acid−aryl ketone complex is partially dissociable, which is both Lewis acid- and temperature-dependent.[3a,b] While it is possible to carry out FC acylations in the presence of some Lewis acids at higher temperatures, this usually provokes side reactions.[3,4] The standard FC workup procedure leads to catalyst destruction and

(1) (a) *Lewis Acids in Organic Synthesis*; Yamamoto, H., Ed.; Wiley-VCH: Weinheim, 2000. (b) *Lewis Acid Reagents: A Practical Approach*; Yamamoto, H., Ed.; Oxford University Press: Oxford, UK, 1999.

(2) (a) *Selectivities in Lewis Acid Promoted Reactions*; Schinzer, D., Ed.; Kluwer Academic Publishers: Dordrecht, Holland, 1989; pp 73–125. (b) Santelli, M.; Pons, J.-M. *Lewis Acids and Selectivity in Organic Synthesis*; CRC: Boca Raton, 1995.

(3) (a) Olah, G. A. *Friedel-Crafts and Related Reactions*, 4th ed.; Interscience: New York, 1964; Vol *2*, Part 2, Chapter 2. (b) Olah, G. A. *Friedel-Crafts and Related Reactions*, 4th ed.; Interscience: New York, 1964; Vol. 3, Part. 2, Chapter 36. (c) Nightingale, D. V. *Chem. Rev.* **1939**, *25*, 329–376.

(4) Taylor, R. *Electrophilic Aromatic Substitution*; John Wiley & Sons: New York, 1990; Chapter 6.

10.1021/jo800158k CCC: $40.75 © 2008 American Chemical Society
Published on Web 04/30/2008

to the formation of large amounts of acid and metal waste.[3,4] In addition, sluggish reaction conditions and the excessive amounts of organic solvents required in workup procedures and in product isolation are environmentally problematic for FC reactions with classical Lewis acids.[3,4]

As a promising means to address the aforementioned issues with conventional Lewis acids, notable progress has been made in the past few decades.[5,6] Among the newly emerged FC acylation catalyst such as binary Lewis acid mixtures,[5a–c] air-stable late transition-metal catalysts,[5f] new types of environmentally friendly f-element Lewis acids, lanthanide trifluoromethanesulfonates, $Ln(OTf)_3$, stand out.[6,7b–d,8,9] Lanthanide ions have far larger ionic radii and formal coordination numbers than typical transition metal ions.[7a–c] They are expected to act as very strong Lewis acids because of their hard, electrophilic character and yet are relatively stable to hydrolysis.[7a–c,8,9] Moreover, the strongly electron-withdrawing properties of the triflate counterion suggest it will act as a good leaving group, as is typical of its role in numerous organic transformations.[6,8b,10] Furthermore, lanthanide triflates remain catalytically active in the presence of many oxygen-, nitrogen-, phosphorus-, and sulfur-containing Lewis bases.[7b–d] In most cases, only substoichiometric (catalytic) quantities of triflate reagents are sufficient to effect useful catalytic transformations.[6,7b–d,9] Importantly, rare earth metal triflates can be easily recovered after reaction completion and recycled without significant loss of activity.[6,7b–d,9]

Lanthanide triflates are employed effectively in a wide range of carbon−carbon bond-forming transformations in aqueous, organic, and biphasic reaction media in which their oxophilicity and regioselectivity have been exploited extensively.[6,7d] Kobayashi and co-workers have studied the application of lanthanide triflates as catalysts in organic transformations such as Aldol reactions, Diels–Alder, retro and aza Diels–Alder reactions, allylation, etc.[6,7,9] While the above reactions proceed readily in water or in biphasic media, Friedel–Crafts acylation mediated by lanthanide triflates proceeds only in organic solvents and ionic liquids.[6,11,12] Our attention was drawn to the application of lanthanide triflates in intermolecular FC acylation, a fundamental reaction in organic synthesis and one of great utility in preparing precursors to many natural products such as aromatic ketones and related structural variants such as indanones, tetralones, hydrindones, etc.[13a,d] These structural motifs play major roles in the medicinal, pharmaceutical, and polymer industries.[13]

In comparison to classical Lewis acids, lanthanide triflate-mediated acylation processes do not require rigorously anhydrous reaction conditions since these are water-tolerant Lewis acids.[6,9,11b] Furthermore, only substoichiometric amounts of catalyst are sufficient for complete conversions, and catalysts can be readily recovered from the aqueous layer after workup, without catalytic activity loss.[6,9,11b] $Ln(OTf)_3$ complexes effectively and selectively catalyze FC acylations in standard organic media and most efficiently in polar nitromethane.[5f,11b] The scope of these catalytic systems has been extensively explored by Kobayashi and co-workers, generally using acid anhydrides as acylation agents and electron-rich aromatic substrates such as anisole.[11b] The final product is a single regioisomer in excellent yield, with efficiency alterable either by increasing the catalyst loading to stoichiometric levels or by introducing a cocatalyst such as $LiClO_4$, which promotes acylation of less reactive aromatics, such as xylenes and toluene, but in certain cases alters the regioselectivity.[14] The catalytic activities of metal triflates can also be enhanced by the addition of triflic acid and the use of acid chlorides as acylating reagents.[15] Since triflic acid is a known catalyst for these reactions, the role of the lanthanide center remains unclear in this case.

To date, little is known about the actual mechanism of $Ln(OTf)_3$-mediated Friedel–Crafts acylation, and there have been no kinetic or mechanistic studies to probe the role of the $Ln(OTf)_3$ catalyst and the interactions/transformations leading to C−C bond formation. It is known that arenes form π-complexes with electrophilic ions such as Sm^{3+}[16] and Ag^{+}[17] and with neutral acceptors such as iodine,[18] so a goal here is to define the nature of the interaction between the Ln^{3+} center and

(5) (a) Izumi, J.; Mukaiyama, T. *Chem. Lett.* **1996**, 739–740. (b) Hachiya, I.; Moriwaki, M.; Kobayashi, S. *Bull. Chem. Soc. Jpn.* **1995**, *68*, 2053–2060. (c) Suzuki, K.; Kitagawa, H.; Mukaiyama, T. *Bull. Chem. Soc. Jpn.* **1993**, *66*, 3729–3734. (d) Mukaiyama, T.; Ohno, T.; Nishimura, T.; Suda, S.; Kobayashi, S. *Chem. Lett.* **1991**, 1059–1062. (e) Mukaiyama, T.; Nagaoka, H.; Ohshima, M.; Murakami, M. *Chem. Lett.* **1986**, 165–169. (f) Fürstner, A.; Voigtländer, D.; Schraider, W.; Giebel, D.; Reetz, M. T. *Org. Lett.* **2001**, *3*, 417–420.

(6) Reviews of $Ln(OTf)_3$-mediated reactions: (a) Li, C.-J.; Chen, L. *Chem. Soc. Rev.* **2006**, *35*, 68–82. (b) Luo, S.; Zhu, L.; Ralukdar, A.; Zhang, G.; Mi, X.; Chen, J.-P.; Wang, P. G. *Mini-Rev. Org. Chem.* **2005**, *2*, 177–202. (c) Li, C. *Chem. Rev.* **2005**, *105*, 3095–3165. (d) Kobayashi, S. *Chem. Rev.* **2002**, *102*, 2227–2302. (e) Kobayashi, S.; Manabe, K. *Acc. Chem. Res.* **2002**, *35*, 209–217. (f) *Topics in Organometallic Chemistry. Lanthanides: Chemistry and Use in Organic Synthesis*; Kobayashi, S., Ed.; Springer-Verlag: Berlin, 1999; Vol. 2, Chapter 2.

(7) Lanthanide chemistry: (a) Imamoto, T. *Lanthanides in Organic Synthesis*; Academic Press: San Diego, 1994. (b) Cotton, S. *Lanthanide and Actinide Chemistry*; Wiley: Chichester, England, 2006. (c) Aspinall, H. C. *Chemistry of the f-Block Elements*; Gordon and Breach Publishers: Amsterdam, 2001. (d) *Aqueous-Phase Organometallic Catalysis*; Cornils, B., Herrmann, W. A., Eds.; Wiley-VCH: New York, 1998.

(8) (a) Molander, G. A. *Chem. Rev.* **1992**, *92*, 29–68. (b) Lawrence, G. *Chem. Rev.* **1986**, *86*, 17–33.

(9) $Ln(OTf)_3$-mediated C−C bond-forming reactions: (a) Kobayashi, S.; Hachiya, I. *J. Org. Chem.* **1994**, *59*, 3590–3596. (b) Engberts, J. B. F. N.; Wijnen, J. W. *J. Org. Chem.* **1997**, *62*, 2039–2044. (c) Bellucci, C.; Cozzi, P. G.; Umani-Ronchi, A. *Tetrahedron Lett.* **1995**, *36*, 7289–7292.

(10) (a) Parker, D.; Dickins, R.; Puschmann, H.; Crossland, C.; Howard, J. *Chem. Rev.* **2002**, *102*, 1977–2010. (b) Kobayashi, S.; Nagayama, S.; Busujima, T. *J. Am. Chem. Soc.* **1998**, *120*, 8287–8288. (c) Baes, C. F.; Mesmer, R. E. *The Hydrolysis of Cations*; Wiley: New York, 1976.

(11) $Ln(OTf)_3$-mediated FC acylation in organic solvents: (a) Kawada, A.; Mitamura, S.; Matsuo, J.; Kobayashi, S. *Bull. Chem. Soc. Jpn.* **2000**, *73*, 2325–2333. (b) Kawada, A.; Mitamura, S.; Kobayashi, S. *J. Chem. Soc., Chem. Commun.* **1993**, 1157–1158.

(12) $Ln(OTf)_3$-mediated FC acylation in ionic liquids (ILs): (a) Hardacre, C.; Katdare, S. P.; Milroy, D.; Nancarrow, P.; Rooney, D. W.; Thompson, J. M. *J. Catal.* **2004**, *227*, 44–52. (b) Xiao, J.; Ross, J. *Green Chem.* **2002**, *4*, 129–133.

(13) Examples of FC acylation used in natural product synthesis: (a) Jackson, W. J. *Macromolecules* **1983**, *16*, 1027–1033. (b) Goudie, A. C.; Gaster, L. M.; Lake, A. W.; Rose, C. J.; Freeman, P. C.; Hughes, B. O.; Miller, D. *J. Med. Chem.* **1978**, *21*, 1260–1264. (c) Crenshaw, R. R.; Luke, G. M.; Bialy, G. *J. Med. Chem.* **1972**, *15*, 1179–1180. (d) Harrison, I. T.; Lewis, B.; Nelson, P.; Rooks, W.; Roszkowski, A.; Tomolonis, A.; Fried, J. H. *J. Med. Chem.* **1970**, *13*, 203–205.

(14) Properties of $LiClO_4$: (a) Malona, J. A.; Colbourne, J. M.; Frontier, A. J. *Org. Lett.* **2006**, *8*, 5661–5664. (b) Komoto, I.; Kobayashi, S. *Tetrahedron Lett.* **2000**, *56*, 6463–6465. (c) Nesakumar, E. J.; Sankararaman, S. *Eur. J. Org. Chem.* **2000**, *11*, 2003–2001. (d) Kawada, A.; Mitamura, S.; Kobayashi, S. *Chem. Commun.* **1996**, 183–184. (e) Hachiya, I.; Moriwaki, K.; Kobayashi, S. *Tetrahedron Lett.* **1995**, *36*, 409–412. (f) Ayerbe, M.; Cossío, F. P. *Tetrahedron Lett.* **1995**, *36*, 4447–4450. (g) Mukaiyama, T.; Suzuki, K.; Han, J.-S.; Kobayashi, S. *Chem. Lett.* **1992**, *3*, 435–438.

(15) TfOH-mediated FC acylation: Dumeunier, R. D.; Markó, I. *Tetrahedron Lett.* **2004**, *45*, 825–829.

(16) Ln^{3+}−arene complexes: (a) Liang, H.; Shen, Q.; Guan, J.; Lin, Y. *J. Organomet. Chem.* **1994**, *474*, 113–116. (b) Deacon, G. B. *Aust. J. Chem.* **1990**, *43*, 1245–1257. (c) Fan, B.; Shen, Q.; Lin, Y. *J. Organomet. Chem.* **1989**, *376*, 61–66. (d) Fan, B.; Shen, Q.; Lin, Y. *J. Organomet. Chem.* **1989**, *377*, 51–58. (e) Cotton, A.; Schwotzer, W. *Organometallics* **1987**, *6*, 1275–1279. (f) Cotton, A.; Schwotzer, W. *J. Am. Chem. Soc.* **1986**, *108*, 4657–4568.

(17) Ag^{+}−arene complexes: Keffer, R. M.; Andrews, J. *J. Am. Chem. Soc.* **1952**, *74*, 640–643.

(18) I_2−arene complexes: Keefer, R. M.; Andrews, L. *J. Am. Chem. Soc.* **1955**, *77*, 2164–2168.

substrate and to better define the sequence of events leading to these facile, lanthanide-mediated arene functionalizations. For the present study, we chose anisole acylation as the representative reaction under the same reaction conditions as employed by Kobayashi et al. (eq 1).[11b] Herein, we present a detailed

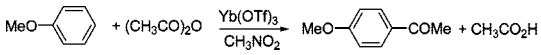

(1)

kinetic/mechanistic investigation of this reaction with the aim of elucidating the role of the Ln^{3+} center in Friedel–Crafts anisole acylation with acetic anhydride. Substrate−Ln^{3+} interactions are investigated using long-T_{1e} and dipolar shift paramagnetic probes. Factors affecting reaction rates such as lanthanide ionic radius, arene substituents, kinetic isotope effects, and the role of $LiClO_4$ cocatalyst are investigated. Finally, these mechanistic observations are compared and contrasted with what is known from classical Friedel–Crafts acylation.

Results

This section begins with a discussion of the reaction kinetics and rate law for $Ln(OTf)_3$-mediated anisole acylation with acetic anhydride. This includes analysis of molecularity, activation parameters, and the CH/CD kinetic isotope effect. We then explore solvent effects, the effects of $Ln(OTf)_3$, substrate variation and $LiClO_4$ cocatalyst effects, and Ln^{3+}−substrate interactions using long-T_{1e} $4f^7$ and dipolar shift paramagnetic probes.

General Reaction Procedure. Preliminary studies of $Ln(OTf)_3$-mediated anisole acylations by acetic anhydride were carried out in the presence of air and moisture to ensure agreement with the literature results.[11b] The stoichiometry used in these initial reactions was $Ln(OTf)_3$:anisole:acetic anhydride = 1:5:10, respectively, at 50 °C for 18 h in nitromethane. Upon completion, the catalyst was recovered from the aqueous phase on workup. The only product detected is the para regioisomer, 4-methoxyacetophenone, and it was characterized by ^{1}H NMR spectroscopy.

Kinetic Studies of Anisole Acylation. Most kinetic data acquired in this study were obtained using $Yb(OTf)_3$ as the precatalyst. The rationale for this choice is that Yb^{3+} exhibits the largest turnover frequencies among the lanthanide triflates examined, and the relatively short Yb^{3+} T_{1e} allows convenient and informative in situ NMR monitoring of the reaction without the excessive line-broadening induced by some other lanthanides (e.g., Figure 1).[19a] The former also allows greater efficiency in kinetic data acquisition and greater accuracy in integration. To minimize potential artifacts, the solvent and substrates used were rigorously purified by distillation under reduced pressure, dried over an appropriate drying agent, and stored under argon (see Experimental Section for more details). For each kinetic data set, a standard solution was prepared. All reaction components were transferred to J-Young NMR tubes under an argon atmosphere on a high-vacuum line to minimize exposure to air and moisture. Quantitative kinetic studies were carried out using in situ ^{1}H NMR spectroscopy at 50 °C, by monitoring reactant consumption as a function of time. For example, catalyst and anisole concentrations were initially held constant, with the anisole:anhydride ratio held to greater than 1:10 (pseudofirst-order in anhydride). The catalyst:anisole ratio was then held at 1:4, and the anisole concentration monitored until ∼90% consumption. The disappearance of the ^{1}H NMR anisole OCH_3 resonance ($\delta \sim 3.84$ ppm) and appearance of the *p*-methoxyacetophenone OCH_3 resonance ($\delta \sim 4.1$ ppm) were normalized to an internal (1,1,2,2-tetrachloroethane) standard ($\delta \sim 6.2$ ppm; Figure 1). In situ ^{1}H NMR analysis of all $Yb(OTf)_3$-mediated acylations indicates that, within the detection limits, only substrate and product are present in detectable quantities at all stages of conversion. Monitoring the reaction for at least 3 turnovers gives initial rate constants for each concentration. For example, a van't Hoff plot of ln k_{obs} versus the ln[anisole] reveals a linear relationship consistent with a first-order dependence (0.936 ± 0.036) in anisole concentration (Figure 2a). The same trend is observed for the dependence of k_{obs} on the concentration of acetic anhydride and $Yb(OTf)_3$ (Figure 2 b,c). Combining all of these results, the overall experimental kinetic order for $Yb(OTf)_3$-mediated acylation of anisole with acetic anhydride is third-order, first-kinetic order in each of the reactants and the catalyst: $\nu \sim k_3[Ln^{3+}]^1[Ac_2O]^1[anisole]^1$.

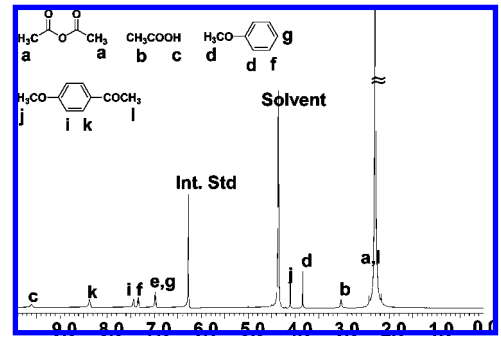

FIGURE 1. Representative 500 MHz ^{1}H NMR spectrum of the reaction for kinetic studies of the $Yb(OTf)_3$-catalyzed acylation of anisole with acetic anhydride with 1,1,2,2-tetrachloroethane as the internal standard in nitromethane-d_3 at 50 °C.

Activation Parameters. To obtain activation parameters, the temperature dependence of the acylation rates was studied, within the practical temperature limits imposed by the system. The rate of $Yb(OTf)_3$-catalyzed acylation was monitored by ^{1}H NMR spectroscopy over a 30–80 °C temperature range, and results are summarized in Table 1. Standard Eyring and Arrhenius kinetic analyses[20] (Figure 3) afford the following activation parameters: $\Delta H^{\ddagger} = 12.9$ (4) kcal·mol^{-1}, $\Delta S^{\ddagger} = -44.8$ (1.3) e.u., and $Ea = 13.1$ (4) kcal·mol^{-1}.

Kinetic Isotope Effects. Three kinetic runs were performed with normal anisole and three runs, under identical conditions with [4-^{2}H]anisole (see Experimental section). Analysis of kinetic data (Table 2) obtained in these experiments indicates a substantial primary KIE, $k_H/k_D = 2.6 \pm 0.15$ (see more in Discussion section below).

Solvent Effects. The effect of reaction medium on the catalytic activity of $Yb(OTf)_3$-mediated anisole acylation with acetic anhydride was also explored (Table 3). When nitromethane or acetic anhydride are used as a solvent, the reaction proceeds smoothly. However, in water, no product formation is observed over 48 h at 50 °C. The product percent yield in neat acetic anhydride is lower, versus that in nitromethane, owing possibly to competition of acetic anhydride with anisole

(19) Ln^{3+}-induced line-broadening: (a) Bertini, I.; Luchinat, C. *Coordination Chemistry Reviews: NMR of Paramagnetic Substances;* Lever, A. B. P., Ed.; Elsevier: Netherlands, 1996; Vol. 150, Chapters 1–9. (b) Nolan, S.; Marks, T. J. *J. Am. Chem. Soc.* **1989**, *111*, 8538–8540. (c) Glavincevski, B.; Brownstein, S. *J. Org. Chem.* **1982**, *47*, 1005–1007.

(20) More, P. M.; Spencer, M. D.; Wilson, S. R.; Girolami, G. S. *Organometallics* **1994**, *13*, 1646–1655.

TABLE 1. Variable-Temperature Kinetic Experiments Rate Constants[a]

temp (K)	$k_{1,obs}$ (min^{-1})	$k_{1,obs}$ (s^{-1})	$k_{3,obs}$	$\ln(k_3/T)$	$\ln(k_3)$	$1/T$
303.15 ± 1	0.0082	1.3667×10^{-4}	5.5449×10^{-7}	−20.1194	−14.4052	3.2987×10^{-3}
313.15 ± 1	0.0143	2.3833×10^{-4}	9.6695×10^{-7}	−19.5958	−13.8491	3.1933×10^{-3}
323.15 ± 1	0.0254	4.2333×10^{-4}	1.7175×10^{-6}	−19.0528	−13.2746	3.0945×10^{-3}
333.15 ± 1	0.0531	8.8501×10^{-4}	3.5907×10^{-6}	−18.3458	−12.5371	3.0016×10^{-3}
353.15 ± 1	0.1575	2.6250×10^{-3}	1.0650×10^{-5}	−17.3168	−11.4499	2.8317×10^{-3}

[a] Reaction conditions: [acetic anhydride] = 2.2 M, [anisole] = 0.138 M, [$Yb(OTf)_3$] = 0.0294 M, [1,1,2,2-tetrachloroethane] = 0.3245 M in nitromethane-d_3.

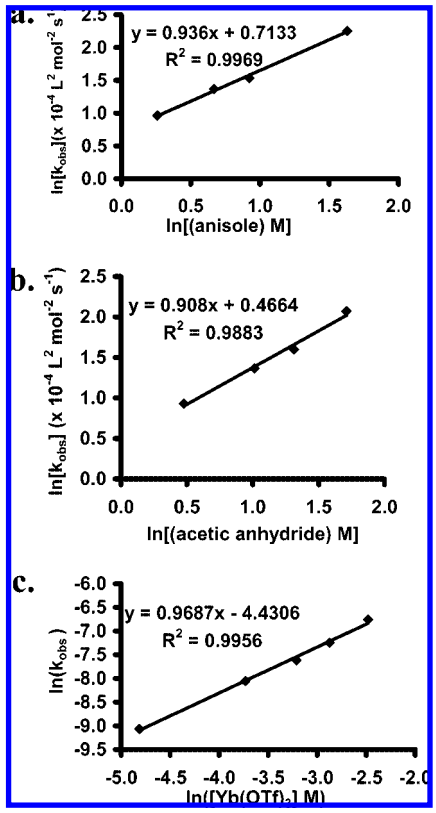

FIGURE 2. (a) van't Hoff plot of ln[k_{obs}] vs ln[anisole] concentration for catalytic production of 4-methoxyacetophenone. Reaction conditions: [acetic anhydride] = 0.14 M, [$Yb(OTf)_3$] = 0.069 M, [1,1,2,2-tetrachloroethane] = 0.26 M in nitromethane-d_3 at 50 °C, $R^2 = 0.9969$. (b) van't Hoff plot of ln[k_{obs}] vs ln[acetic anhydride] for catalytic production of 4-methoxyacetophenone. Reaction conditions: [anisole] = 0.14 M, [$Yb(OTf)_3$] = 0.069 M, [1,1,2,2-tetrachloroethane] = 0.25 M in nitromethane-d_3 at 50 °C, $R^2 = 0.9883$. (c) van't Hoff plot of ln[k_{obs}] vs ln[$Yb(OTf)_3$] concentration for catalytic production of 4-methoxyacetophenone. Reaction conditions: [acetic anhydride] = 2.5 M, [anisole] = 0.24 M, [1,1,2,2-tetrachloroethane] = 0.26 M in nitromethane-d_3 at 50 °C, $R^2 = 0.9956$.

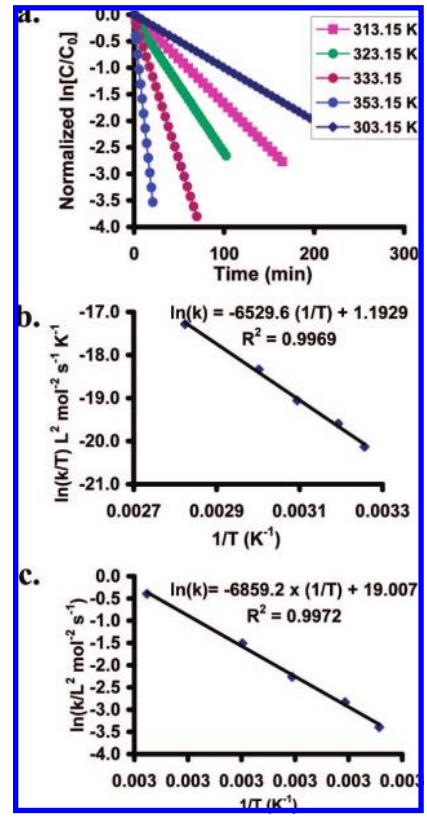

FIGURE 3. (a) Plot of acylation rate constants as a function of temperature. (b) Eyring plot for $Yb(OTf)_3$-mediated anisole acylation with acetic anhydride in nitromethane-d_3. (c) Arrhenius plot for $Yb(OTf)_3$-mediated anisole acylation with acetic anhydride in nitromethane-d_3. The lines are least-squares fits to the data points.

for coordination at the metal center (see more in Discussion section below).

Effect of Ln^{3+} Ionic Radius on Reaction Efficiency and Turnover Frequencies. A catalytic rate dependence on metal ion size was previously observed for classical Friedel–Crafts acylation processes, with $AlCl_3$ being the smallest and most effective catalyst. The effect of lanthanide variation on $Ln(OTf)_3$-mediated anisole acylation by acetic anhydride on reaction efficiency was probed in nitromethane at 50 °C under rigorously anhydrous, anaerobic conditions. In the present study, the most active catalyst is found to be $Yb(OTf)_3$ (Table 4), with efficiency scaling inversely with Ln^{3+} ionic radius, while the regioselectivity remains constant. The results obtained are similar to those reported in the literature conducted under less rigorous anhydrous/anaerobic conditions.[11b] The formation of the ortho product isomer is not observed in the ^1H NMR spectrum, indicative of exclusive para-selectivity. Moving across the lanthanide series, for fixed reaction time, turnover frequency increases with increasing Lewis acidity of the lanthanide ion[7a–c] (Tables 4 and 5, Figure 4; see more in Discussion section below).

Substrate Substituent and Cocatalyst Effects. Arene substituent effects on acylation rates and regioselection were investigated under the present anhydrous/anaerobic $Yb(OTf)_3$-mediated reaction conditions (eq 2). Several substituted benzenes were subjected to $Yb(OTf)_3$-catalyzed acylation with acetic anhydride (Table 6). Reactions occurring with non-negligible rates produced a single acylated product, and the formation of other isomers was not observed by ^1H NMR analysis. It is known that this catalytic system generally turns over only with

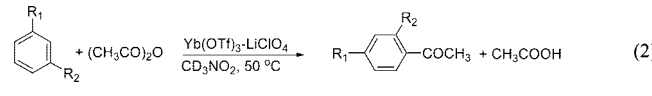

(2)

TABLE 2. Rate Constants Obtained from the Least-Squares Fits to Experimental Data Used in Determination of the Kinetic Isotope

trial	k_H (s^{-1})	σ^a $k_H \times 10^{-3}$	k_D (s^{-1})	$\sigma^a k_D \times 10^{-4}$
1	1.228×10^{-3}	($\pm$0.021)	4.683×10^{-4}	($\pm$0.023)
2	1.286×10^{-3}	($\pm$0.037)	4.867×10^{-4}	($\pm$0.161)
3	1.235×10^{-3}	($\pm$0.014)	4.567×10^{-4}	($\pm$0.139)
mean	1.249×10^{-3}	($\pm$0.031)	4.706×10^{-4}	($\pm$0.151)

[a] Standard deviation associated with each measurement and the average.

TABLE 3. Reaction Medium Effects on Yb(OTf)$_3$-Mediated Anisole Acylation with Acetic Anhydride

solvent	ε^d	reaction conditions	reaction time	product % yield[e]
CD_3NO_2	36.4	50 °C	24 h	98
H_2O[a]	80.4	50 °C	48 h	[b]
Ac_2O[c]	21.0	50 °C	24 h	57

[a] Entry 2 uses neat water. [b] Product formation was not observed. [c] Entry 3 uses neat acetic anhydride. [d] Solvent dielectric constant at 25 °C. [e] Product percent yield. Reaction conditions: [acetic anhydride] = 0.8 M, [anisole] = 0.4 M, [Yb(OTf)$_3$] = 0.08 M at 50 °C, 24 h.

TABLE 4. Effect of Lanthanide(III) Ionic Radius on Anisole Acylation with Acetic Anhydride

Ln(OTf)$_3$	ionic radius M^{3+}, Å	product yield (%)[a]	N_t (h^{-1})	(%) catalyst recovered[a]
La	1.172	37	1.73	93
Sm	1.098	75	3.45	90
Eu	1.087	82	3.74	95
Yb	1.008	95	4.99	93

[a] Catalyst recovered from the aqueous layer in product isolation workup and dried on a Schlenk line under vacuum at 100 °C for 24 h. Reaction conditions: [Ln(OTf)$_3$] = 0.070 M, [anisole] = 0.38 M, [acetic anhydride] = 0.72 M, [1,1,2,2-tetrachloroethane] = 0.49 M in nitromethane-d_3 at 50 °C, 18 h reaction time.

TABLE 5. Correlation between Ln(OTf)$_3$-Mediated Anisole Acylation Rate Constants and Ln^{3+} Ionic Radius

catalyst	ionic radius M^{3+}, Å	k_{obs} (s^{-1})[a]
La(OTf)$_3$	1.172	2.20×10^{-4}
Eu(OTf)$_3$	1.087	3.58×10^{-4}
Yb(OTf)$_3$	1.008	4.92×10^{-4}
Lu(OTf)$_3$	1.001	8.98×10^{-4}

[a] Reaction conditions: [acetic anhydride] = 1.35 M, [anisole] = 0.14 M, [Ln(OTf)$_3$] = 2.94×10^{-2} M, and [1,1,2,2,-tetrachloroethane] = 0.222 M in nitromethane-d_3, 50 °C.

strongly electron-donating arene substituents for which the rate constants were obtained in the present study. No rate data were obtained in the acylation of *N*,*N*-dimethylaniline. The ordering of substituent effects on the rate of Yb(OTf)$_3$-promoted acylation is $OCH_3 > SCH_3 >> (CH_3)_2 \approx N(CH_3)_2$. The results are summarized in Table 6.

It has been reported that the presence of a $LiClO_4$ cocatalyst further enhances acylation rates of even less reactive aromatics, and the role of $LiClO_4$ appears to be limited to enhancing Ln(OTf)$_3$ efficiency since $LiClO_4$ alone does not promote the reaction.[14] Therefore, potential cocatalyst effects were investigated as well. Indeed, the presence of 6.0 equiv of $LiClO_4$ promotes arene acylation with less electron-donating groups such as *m*-xylene. However, acylation of *N*,*N*-dimethylaniline was immeasurably sluggish even under these conditions (see Discussion section below). The effects of $LiClO_4$ on the acylation rates of arenes with acetic anhydride using the Yb(OTf)$_3$−$LiClO_4$ catalytic system are summarized in Table 6.

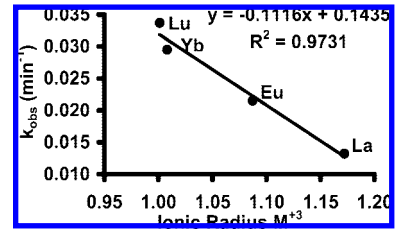

FIGURE 4. Effect of Ln^{3+} ionic radius on k_{obs} for anisole acylation with acetic anhydride in nitromethane-d_3 at 50 °C.

TABLE 6. Arene Substituent Effects on Yb(OTf)$_3$-Mediated Arene Acylation with Acetic Anhydride with and without the Presence of $LiClO_4$ as a Cocatalyst

entry	R^1	R^2	catalyst	cocatalyst	k_{obs} (s^{-1})
1[a]	OCH_3	H	Yb(OTf)$_3$	-	1.57×10^{-3}
2[b]	OCH_3	H	Yb(OTf)$_3$	$LiClO_4$	3.80×10^{-3}
3[a]	SCH_3	H	Yb(OTf)$_3$	-	1.03×10^{-4}
4[b]	SCH_3	H	Yb(OTf)$_3$	$LiClO_4$	1.84×10^{-4}
5[a]	$N(CH_3)_2$	H	Yb(OTf)$_3$	-	[c]
6[b]	$N(CH_3)_2$	H	Yb(OTf)$_3$	LiClO4	[d]
7[a]	CH_3	CH_3	Yb(OTf)$_3$	-	[c]
8[b]	CH_3	CH_3	Yb(OTf)$_3$	$LiClO_4$	1.39×10^{-5}

[a] Reaction conditions: [acetic anhydride] = 1.35 M, [Yb(OTf)$_3$] = 6.9×10^{-2} M, and [1,1,2,2-tetrachloroethane] = 0.222 M in nitromethane-d_3, 50 °C. [b] Reaction conditions: [acetic anhydride] = 1.35 M, [Yb(OTf)$_3$] = 6.9×10^{-2} M, [$LiClO_4$] = 0.41 M, and [1,1,2,2-tetrachloroethane] = 0.222 M in nitromethane-d_3, 50 °C. [c] No product formation observed by ^{1}H NMR. [d] Desired product formation was not observed. Instead, a gelatinous sludge formed at the beginning of the reaction with an unresolved ^{1}H NMR spectrum.

Coordinative Probing. While kinetic studies provide the overall reaction order and suggest the turnover-limiting step, NMR line-broadening experiments give qualitative insight into which substrate and product species enter the Ln^{3+} coordination sphere.[19] The first set of experiments consisted of adding small increments of paramagnetic Gd(OTf)$_3$ to a 6.36 M solution of acetic anhydride in nitromethane-d_3 (Figure 5). Resonance line width at half-height ratios obtained from individual peak measurements indicate significantly larger line-broadening of the acetic anhydride resonance versus that of the nitromethane peak, suggesting preferential Ln^{3+}−acetic anhydride complexation (for acetic anhydride/nitromethane line width at half-height ratios, see Figure 5). In the second set of experiments, small increments of paramagnetic Gd(OTf)$_3$ are added to a solution containing both anisole and acetic anhydride, and then differences in paramagnetically induced ^{1}H NMR line-broadening observed (Figure 6; see Discussion section below on Ln^{3+}-Substrate Interactions and the Nature of the Active Species). Resonance line width at half-height ratios derived from individual measurements of acetic anhydride and arene peaks indicate some preferential line-broadening of the acetic anhydride versus arene aromatic resonances (for ratios, see Figure 6).

In a third set of coordinative probe experiments, small increments of Gd(OTf)$_3$ were first loaded into J-Young NMR tubes containing fixed amounts of $LiClO_4$ to which was then added a standard solution containing acetic anhydride, 1,1,2,2-tetrachloroethane, and internal NMR standard, in nitromethane-d_3, and then differences in paramagnetically induced line-broadening in the ^{1}H NMR spectrum were observed. The NMR spectra are indistinguishable from those in the other

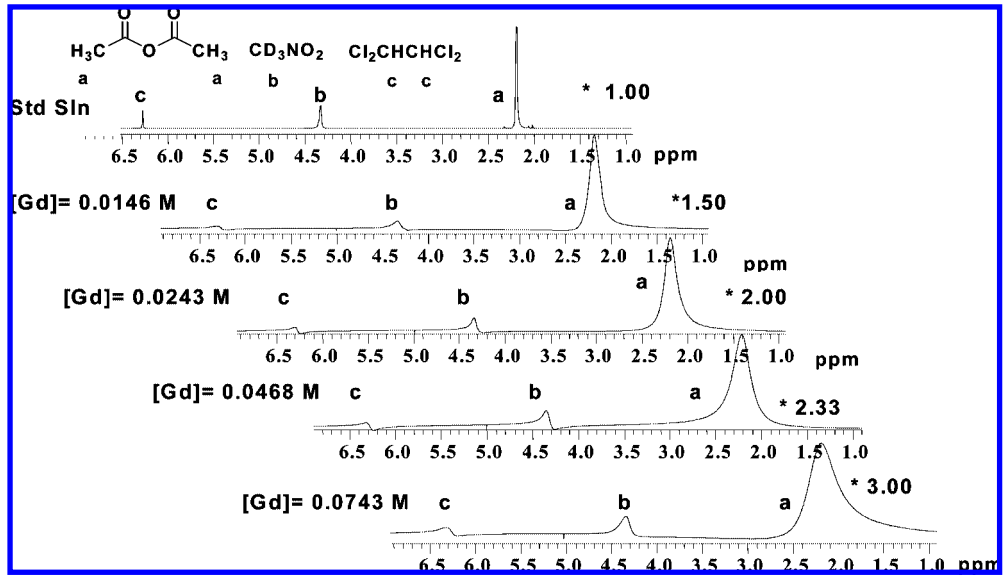

FIGURE 5. Overlaid 500 MHz ^{1}H NMR spectra of solutions having different $Gd(OTf)_3$ concentrations demonstrating the effect of increasing $[Gd(OTf)_3]$ on the line width at half-height ratio of acetic anhydride: nitromethane-d_3. All spectra were recorded at $t = 0$ min. Reaction solution: [acetic anhydride] = 6.36 M, [1,1,2,2-tetrachloroethane] = 0.05 M in nitromethane-d_3 at room temperature. 500 MHz ^{1}H NMR CD_3NO_2: δ 2.219 ppm (a, 3H, s, $(CH_3CO)_2O$), 4.33 ppm (b, CD_3NO_2), 6.269 ppm (c, 2H, s, $Cl_2CHCHCl_2$). * $(CH_3CO)_2O/CD_3NO_2$ line width at half-height ratio.

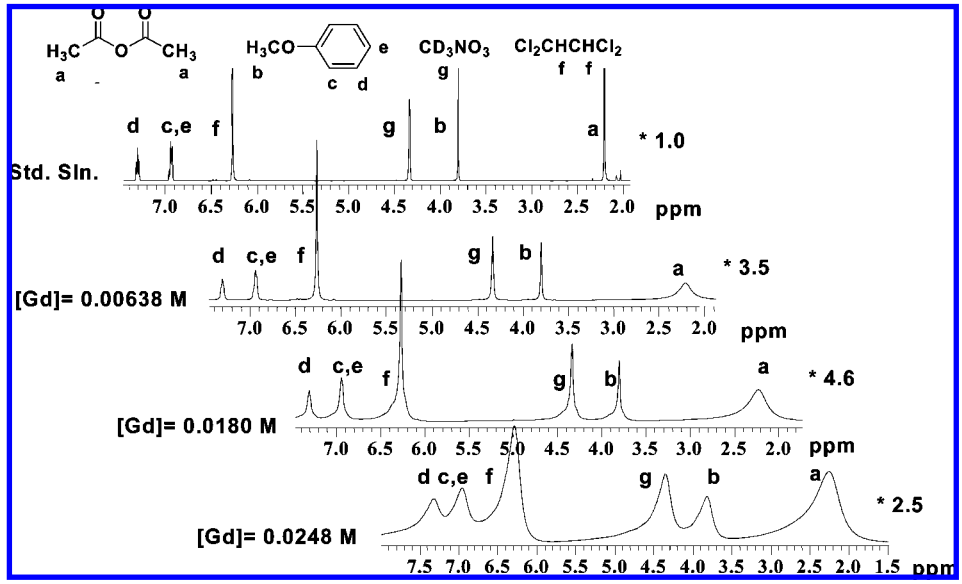

FIGURE 6. Overlaid 500 MHz ^{1}H NMR spectra of the reaction solution having different $Gd(OTf)_3$ concentrations demonstrating the effect of increasing $[Gd(OTf)_3]$ on the line width half-height ratio of acetic anhydride versus anisole. Standard solution: [acetic anhydride] = 0.917 M, [anisole] = 0.131 M, [1,1,2,2-tetrachloroethane] = 0.263 M, in nitromethane-d_3 at room temperature. 500 MHz ^{1}H NMR CD_3NO_2 (g): δ 2.203 ppm (a, 6H, s, $(CH_3CO)_2O$), 3.796 ppm (b, 3H, s, OCH_3), 6.264 ppm (f, 2H, s, $Cl_2CHCHCl_2$), 6.938 ppm (c, 3H, m, ArH), 7.303 ppm (d, 2H, dd, ArH). * Calculated $(CH_3CO)_2O$/ArH line width at half-height ratio.

$Gd(OTf)_3$−acetic anhydride coordination probing experiments shown in Figure 5 (see Discussion section below).

Yb^{3+}−Arene Interaction. To complement the NMR line-broadening studies, additional arrayed experiments were carried out in which in situ monitoring of the course of $Yb(OTf)_3$-mediated acylation with acetic anhydride probed Yb^{3+}−arene interactions via chemical shift changes of the aromatic ^{1}H resonances (Figure 7) (for details, see Experimental section). Yb^{3+} was chosen since it induces reasonably small line-broadening, allowing more accurate peak integration. In the $Yb(OTf)_3$-mediated acylation of anisole and thioanisole with acetic anhydride, substantial changes in the aromatic proton resonance chemical shift dispersion are observed on initiation of reaction (Figure 7). Observation of significant displacements in the acetic anhydride methyl resonance is precluded by the large stoichiometric excess of this reagent (see Figure 7).

Discussion

Molecularity and Rate Law. Early studies of classical FC acylation processes afforded no examples of simple kinetics.[21] The available kinetic data provide ambiguous/conflicting conclusions about the identity of the active electrophile. Rate equations of the form $v = k[RCOCl\cdot AlCl_3]^1\,[ArH]^1$ have been reported for reaction of benzene and toluene with both acetyl and benzoyl chloride.[21a–e] These results are consistent with either

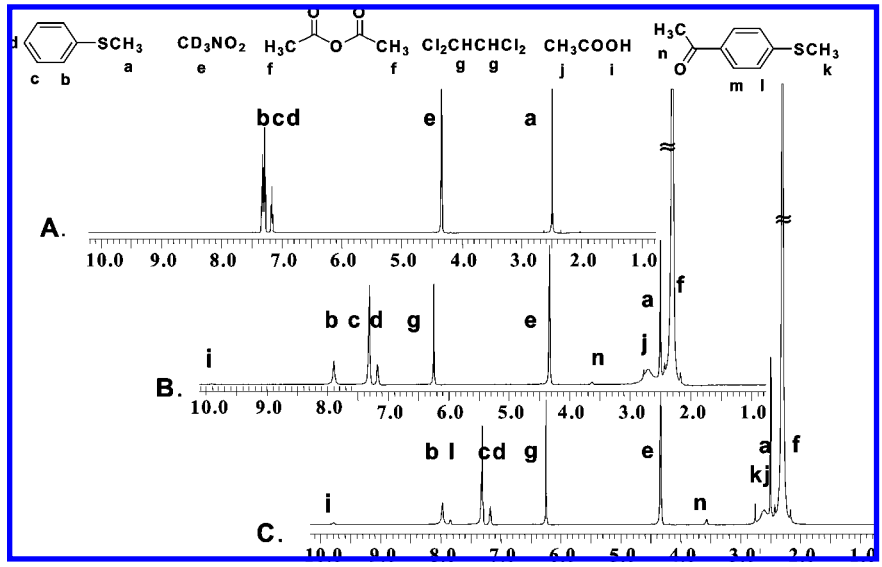

FIGURE 7. (A) 500 MHz ^{1}H NMR spectrum of the thioanisole aromatic region in nitromethane-d_3. (B) 500 MHz ^{1}H NMR spectrum of the thioanisole aromatic region in the reaction mixture at $t = 0$ min of the acylation reaction. (C) 500 MHz ^{1}H NMR spectrum of thioanisole aromatic region at $t = 5$ min of the acylation reaction. Reaction mixture: [acetic anhydride] = 1.45 M, [thioanisole] = 0.138 M, [Yb(OTf)$_3$] = 0.069 M, [1,1,2,2-tetrachloroethane] = 0.3245 M in nitromethane-d_3 at 50 °C.

of two catalytic reaction pathways: via a free acylium ion pair (eqs 3 and 4) or by nucleophilic attack (eqs 5 and 6), with preference for a particular pathway being solvent- and temperature-dependent.[3a,b,4] For reactions that proceed via an acylium ion pair pathway, the overall reaction order is second. The last step, decomposition of the σ-complex is thought to be rate-determining (see Discussion section below on Temperature and Kinetic Isotope Effects), which corresponds to observed rate law (eqs 3 and 4).[3,21e] The acylium ion pair mechanism is preferred by activated aromatics, sterically hindered acylating agents, in polar solvents, and at higher temperatures.[3a,b]

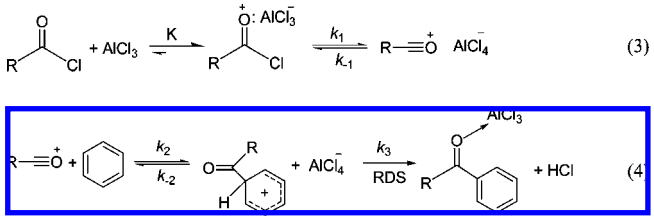

The present kinetic results for Yb(OTf)$_3$-catalyzed anisole acylation with acetic anhydride (see Results section above) clearly indicate the overall empirical rate law of eq 7, first-order kinetics in each of the reactants, and the catalyst.

$$v \sim k_3[\mathrm{Ln}^{3+}]^1[\mathrm{Ac_2O}]^1[\mathrm{anisole}]^1 \qquad (7)$$

The significance of the first-order dependence of the rate upon the aromatic hydrocarbon concentration for this reaction suggests that the turnover-limiting step is not electrophile formation, but the subsequent attack on the aromatic hydrocarbon, which is consistent with observed substituent effects (see Discussion section below).

TABLE 7. Summary of Activation Parameters Obtained in Various Acylation Reactions

catalyst	solvent	$\Delta H^{\ddagger}$ (kcal·mol^{-1})	$\Delta S^{\ddagger}$ (e.u.)	E_a (kcal·mol^{-1})	ref
Yb(OTf)$_3$[a]	CH_3NO_2	12.9 (4)	− 44.8 (1.3)	13.1 (4)	this work
$AlCl_3$[b]	EDC[b]	12.7	− 27.6	13.3	22a
$AlCl_3$[c]	EDC	13.3	− 28.1	13.9	22b
$AlCl_3$[c]	BC[c]	12.8	− 26.7	13.3	21e
$SnCl_4$[d]	BC	10.3	− 48.0	10.9	21e, f

[a] Yb(OTf)$_3$-mediated anisole acylation with acetic anhydride in nitromethane. [b] $AlCl_3$-mediated benzene and toluene acylation with acylchloride in EDC (ethylenedichloride). [c] $AlCl_3$-mediated benzene and toluene acylation with benzoylchloride (BC) neat and in EDC. [d] $SnCl_4$-mediated benzene and toluene neat benzoylation. Note: This work's activation parameters comparison was made to $AlCl_3$-mediated reactions that exhibit second-order kinetics: $v = k_2[AlCl_3 \cdot RCOCl]^1[ArH]^1$, first-order with respect to the $AlCl_3$−acylating agent complex and arene.

Temperature and Kinetic Isotope Effects. Variable-temperature kinetic characterization of Yb(OTf)$_3$-catalyzed anisole acylation with acetic anhydride yields the following activation parameters: $\Delta H^{\ddagger} = 12.9$ (4) kcal·mol^{-1}, $\Delta S^{\ddagger} = -44.8$ (1.3) e.u., and $E_a = 13.1$ (4) kcal·mol^{-1}. These values are comparable to those found in classical $AlCl_3$-catalyzed FC acylation reactions that exhibit overall second-order kinetics of type $v = k_2[AlCl_3 \cdot RCOCl]^1[ArH]^1$.[21c,22] As shown in Table 7, $AlCl_3$-catalyzed benzene acetylation in ethylenedichloride proceeds with $\Delta H^{\ddagger} = 12.7$ kcal·mol^{-1}, $\Delta S^{\ddagger} = -27.6$ e.u., and $E_a = 13.3$ kcal·mol^{-1}.[22a] Similar parameters were reported for both

(21) Classical FC acylation rate laws: (a) DeHaan, F. P.; Covey, W. D.; Delker, G. L.; Baker, N. J.; Feigon, J. F.; Ono, D.; Miller, K. D.; Stelter, A. D. *J. Org. Chem.* **1984**, *49*, 3959–3963. (b) Kirkman, S.; Wolfenden, R. *J. Am. Chem. Soc.* **1978**, *100*, 5944–5955. (c) Kobayashi, S.; Olah, G. A. *J. Am. Chem. Soc.* **1971**, *93*, 6964–6967. (d) Brown, H. C.; Marino, G. *J. Am. Chem. Soc.* **1959**, *81*, 5611–5615. (e) Brown, H. C.; Jensen, F. R. *J. Am. Chem. Soc.* **1958**, *80*, 2291–2296. (f) Brown, H. C.; Jensen, F. R. *J. Am. Chem. Soc.* **1958**, *80*, 3039–3040.

(22) (a) Brown, H. C.; Marino, G. *J. Am. Chem. Soc.* **1959**, *81*, 3310–33114. (b) Jensen, F. R.; Marino, G.; Brown, H. C. *J. Am. Chem. Soc.* **1959**, *81*, 3303–3306.

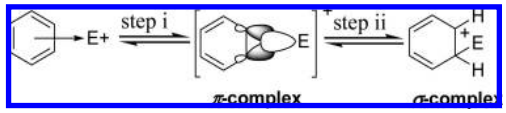

FIGURE 8. Electrophile (E^+) interacts with an aromatic substrate forming a weak reagent−substrate complex. As E^+ approaches the bonding distance, the aromatic HOMO π-orbital overlaps with an empty electrophile orbital, forming a two-electron, three-center π-complex (step i), which leads to σ-complex formation (step ii), followed by final C−H cleavage.[3,4,24]

acetylation and benzoylation of benzene in either ethylene dichloride[22b] or benzoyl chloride as the solvent.[21e] However, $SnCl_4$-catalyzed toluene benzoylation in benzoyl chloride proceeds with a far larger negative activation entropy $\Delta S^{\ddagger} = -48$ e.u. versus $\Delta S^{\ddagger} = -27$ e.u. for toluene benzoylation using $AlCl_3$ as the catalyst.[21e,f] These discrepancies were explained by differences in the strength of benzoyl halide complexation to $AlCl_3$ versus $SnCl_4$.[21e,f] Thus, $SnCl_4$ is not significantly complexed to benzoyl chloride in solution,[21e,f] and the large difference in $\Delta S^{\ddagger}$ values reflects a loss in degrees of freedom accompanying $SnCl_4$−benzoyl chloride complex formation prior to the turnover-limiting step.

Reasoning similar to that for $SnCl_4$ can rationalize the large negative $\Delta S^{\ddagger}$ observed in $Ln(OTf)_3$-mediated acylation, also considering nitromethane solvation effects. Literature reports indicate far greater $Yb(OTf)_3$-mediated anisole acylation rates in polar, moderately coordinating aprotic solvents such as CH_3NO_2 and CH_3CN, rather than in less polar, less coordinating aprotic solvents, such as CH_2Cl_2.[6f,11b] For neutral substrates, such as anisole and acetic anhydride, polar aprotic solvents should accelerate the reaction, due to stabilization of transition state charge separation.[4,23] Therefore, the large negative $\Delta S^{\ddagger}$ is also indicative of a highly organized transition state, plausibly reflecting some combination of loss of degrees of freedom in Ln^{3+}−acetic anhydride complexation, solvent reorganization in stabilizing the charged transition state, and substrate reorganization optimizing Ln^{3+}−arene proximity.

Kinetic hydrogen isotope effects in electrophilic substitutions and their interpretation regarding transition state position along the reaction coordinate have been extensively reviewed.[3,4,24] As noted above in the discussion of classical FC acylation reaction mechanisms, if the step i (Figure 8), electrophilic attack on the arene, is turnover-limiting, the transition state would resemble a π-complex (Figure 8), and a small secondary isotope effect is expected since no C−H bonds are broken or formed.[3,4,24] Examples of electrophilic aromatic substitutions proceeding with secondary isotope effects include nitration where $k_H/k_D = 1.17$.[21c,24−27] However, if the proton elimination is turnover-limiting, the transition state would evolve from a σ-complex (step ii, Figure 8), and a primary isotope effect is expected.[3,4,21c,24−27] Analysis of the present kinetic data yields a primary KIE, $k_H/k_D = 2.6 \pm 0.15$, suggesting that the turnover-limiting step in the $Yb(OTf)_3$-mediated anisole acylation with acetic anhydride is C−H bond cleavage, in general accord with previous KIE observations for other Lewis acid-mediated acetylations.[21c,27]

The magnitude of the present KIE suggests C−H scission is either partial or complete in the transition state.[24,27] These results are consistent with the overall rate law and the multistep mechanism of eqs 8, 9, and 10. In classical FC $AlCl_3$-catalyzed benzene and toluene acetylations in polar nitro solvents, comparable values are: $k_H/k_D = 2.45$ and 2.68, respectively.[21c,22,28]

$$Ln^3 + Ac_2O \underset{k_{-1}}{\overset{k_1}{\rightleftharpoons}} Ln(Ac_2O)^{3+} \quad (8)$$

$$Ln(Ac_2O)^{3+} + \text{anisole} \underset{k_{-2}}{\overset{k_2}{\rightleftharpoons}} Ln(Ac_2O)(\text{anisole})^{3+} \quad (9)$$

$$Ln(Ac_2O)(\text{anisole})^{3+} \xrightarrow{k_3} Ln^{3+} + \text{product} + \text{AcOH} \quad (10)$$

Solvent Effects. Comparative kinetic studies of $Yb(OTf)_3$-mediated anisole acylation with acetic anhydride in different solvents reveal that nitromethane is by far the most effective, followed by acetic anhydride, with water being the least effective (Table 3). While both nitromethane and water have high dielectric constants and large dipole moments (Table 3), the difference lies in the cation-coordinating strength.[21] ^{17}O and ^{19}F NMR studies show that in aqueous solution, $Ln(OTf)_3$ OTf^- anions are displaced by water molecules, which reside in the inner coordination sphere of the hydrated complex.[28] Hydrogen-bonding among the coordinated water molecules further impedes their displacement. The energetic cost of disrupting the H-bonding increases the activation energy of acylation, and moreover, Mackenzie and Winter showed that for $HClO_4$-mediated FC acylation, water rapidly converts acetic anhydride into acetic acid, thus depleting the acylating agent.[29] Therefore, in aqueous solution, formation of the hydrated Ln^{3+} complexes as well as depletion of the acylating agent explain why negligible turnover is observed.

In contrast to water, nitromethane is considered to be a moderately cation-coordinating solvent as reflected by its Ln^{3+} coordination number, 2.7.[23] As noted above, $Gd(OTf)_3$-induced line-broadening effects on acetic anhydride + nitromethane resonances suggest preferential coordination of acetic anhydride versus nitromethane. Therefore, in moderately cation-coordinating nitromethane, substrate competition for Ln^{3+} coordination is not severe, thus allowing precatalyst activation and catalytic turnover. Modest product yields in neat acetic anhydride versus nitromethane possibly reflect competition of acetic anhydride with anisole for coordination at the Ln^{3+} center (see Results, Table 3).

Lewis Acidity Effects. In the cases of $AlCl_3$, BF_3, and $TiCl_4$-catalyzed acylations, the kinetic order in catalyst depends on

(23) Reichardt, S. *Solvents and Solvent Effects in Organic Chemistry*; Wiley-VCH: Weinheim, 1990.

(24) Melander, L.; Sanders, W. H. *Reaction Rates of Isotopic Molecules*; John Wiley & Sons: New York, 1980.

(25) Covalent $AlCl_3$ complexes: (a) Bigi, F.; Casnati, G.; Sartori, G.; Predieri, G. *J. Chem. Soc., Perkin Trans. 2* **1991**, 1319–1321. (b) Chevrier, B.; Weiss, R. *Angew. Chem., Int. Ed. Engl.* **1974**, *13*, 1–10. (c) Chevrier, B.; Le Carpentier, J.-M.; Weiss, R. *J. Am. Chem. Soc.* **1972**, *94*, 5718–5723.

(26) Ionic $AlCl_3$ complexes: (a) Xu, T.; Barich, D. H.; Torres, P. D.; Nicholas, J. B.; Haw, J. F. *J. Am. Chem. Soc.* **1997**, *119*, 396–405. (b) Boer, F. P. *J. Am. Chem. Soc.* **1968**, *90*, 6706–6709. (c) Olah, G. A.; Kuhn, S. J.; Toglyesi, W. S.; Baker, E. B. *J. Am. Chem. Soc.* **1962**, *84*, 2733–2740. (d) Olah,G. A.; Germain, A.; White, A. M. *Carbonium Ions*; Olah, G. A., Schleyer, P. v. R., Eds.; Wiley: New York, 1976; Vol. 5, pp 2049−2133.

(27) Olah, G. A.; Kuhn, S. J.; Flood, S. J.; Hardie, B. A. *J. Am. Chem. Soc.* **1964**, *86*, 2203–2209.

(28) (a) Campbell, R.; Maraschin, V.; Silber, H. B. *J. Solid State Chem.* **2003**, *171*, 225–229. (b) Zhang, S.; Wu, K.; Biewer, M. C.; Sherry, D. A. *Inorg. Chem.* **2001**, *40*, 4284–4290. (c) van Loon, A. M.; van Bekkum, H.; Peters, J. A. *Inorg. Chem.* **1999**, *38*, 3080–3084. (d) Merbach, A.; Helm, L.; Cossy, C. *Inorg. Chem.* **1998**, *27*, 1973–1979. (e) Swift, T. J.; Connick, R. E. *J. Chem. Phys.* **1962**, *37*, 307–320.

(29) (a) Mackenzie, H. A.; Winter, E. R. S. *Trans. Faraday Soc.* **1948**, *44*, 243–253. (b) Mackenzie, H. A.; Winter, E. R. S. *Trans. Faraday Soc.* **1948**, *44*, 171–181. (c) Mackenzie, H. A.; Winter, E. R. S. *Trans. Faraday Soc.* **1948**, *44*, 159–171.

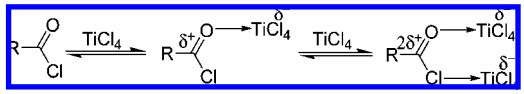

FIGURE 9. Complex formed in polarization of an acyl halide by a Lewis acid such as $TiCl_4$.

the Lewis acid strength. The order in weaker Lewis acids such as $SbCl_5$ or $TiCl_4$ is second, consistent with a requirement for the two molecules to polarize the acyl halide for acylation to occur.[21e,f,30] If a catalyst has greater chloride than oxygen affinity (Figure 9), C−Cl bond weakening is thought to occur, followed by ionization, thus increasing the acylium ion concentration and favoring an acylium ion mechanism (eqs 3 and 4).[3,21e,f,30] The extent of C−Cl bond polarization depends on the Lewis acid strength.[3,30] As shown here, anisole acylations with acetic anhydride mediated by lanthanide triflates (Ln = La, Eu, Yb, Lu) proceed at rates dependent on Ln^{3+} size, with larger ions proceeding more sluggishly (see Results section, Table 5). Moreover, we find that the kinetic order in $[Ln^{3+}]$ across the series is invariant. Weaker Lewis acids such as $TiCl_4$ produce much lower product percent yields than $AlCl_3$.[21e,f,30] The same trend is observed in the present $Ln(OTf)_3$-mediated anisole acylation with acetic anhydride. Moving across the lanthanide series, N_t and product yield increase with increasing Ln^{3+} Lewis acidity (see Results section on Lanthanide Effects on Efficiency and Turnover Frequency; Tables 4 and 5, Figure 4).

Turnover frequency variations as a function of Ln^{3+} ionic radius for lanthanide triflate-mediated anisole acylation are rather modest (see Results section above on Lanthanide Effects on Efficiency and Turnover Frequencies; Table 5, Figure 4). In contrast, for other lanthanide-catalyzed reactions such as aminoalkene hydroamination/cyclization, increasing the Ln^{3+} ionic radius increases the turnover frequency (N_t) markedly (100–1000-fold times N_t increases are not unusual), presumably reflecting significant steric demands in the transition state.[31,32] Combining all of the above observations suggests minimal ionic radius-dependent steric impediments in the acylation transition state.

Arene Substituent Effects. Arene substituent trends observed in the present $Yb(OTf)_3$-mediated acylations parallel classical FC acylations.[3,4,33,34] The present kinetic ordering of aromatic substituents is: OMe > SMe >> $(Me)_2$ > NMe_2. Arenes with methoxy and methylthio are known to accelerate acylation and have been successfully acylated using stoichiometric amounts of many classical Lewis acids such as $AlCl_3$, $TiCl_4$, and $SnCl_4$.[3,4,33,34] In the present catalytic system, the rates of

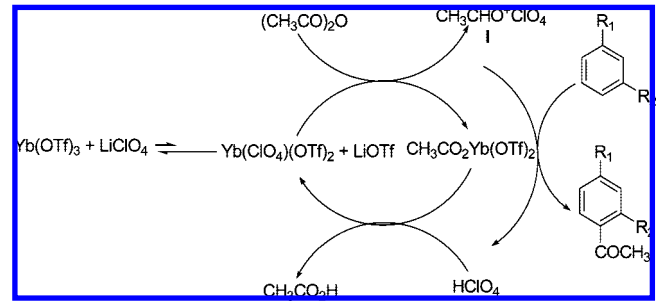

FIGURE 10. Plausible role of $LiClO_4$ as a cocatalyst in $Yb(OTf)_3$−$LiClO_4$ mediated arene acylation with acetic anhydride.

$Yb(OTf)_3$-mediated anisole and thioanisole acylation of are 1.57 × 10^{-3} s^{-1} and 1.03 × 10^{-3} s^{-1}, respectively (Table 6), while methyl substituents generally have little effect on FC arene acylation rates.[34c,f] In this study, *m*-xylene acylation proceeds in the presence of a $LiClO_4$ cocatalyst with a rate constant of 1.3 × 10^{-5} s^{-1} (Table 6; entry 7). *N*,*N*-Dimethylaniline may undergo para acylation with $AlCl_3$, but only traces of ketone are obtained.[34b] The sluggish reactivity of *N*,*N*-dimethylaniline is attributed to strongly deactivating coordination to the catalyst of the basic amine (Table 6, entries 5 and 6).[5f,34b]

Cocatalyst Effects. The results detailed in Table 6 clearly indicate that $LiClO_4$ accelerates the acylation of all substrates examined. A major factor responsible for the acylation rate enhancement is likely the established Lewis acidity of Li^+ in organic solvents, dependent on the solvent basicity and coordinating characteristics, thus facilitating the formation of polar and/or ionic intermediates.[14e,35] An example of solvent–Li^+ Lewis acidity enhancement is found in enhanced rates of aldehyde and cyclic ketone aldol condensation with silyl enol ethers in 5 M $LiClO_4$−CH_3NO_2 versus 5 M $LiClO_4$−Et_2O.[36] Diethyl ether is a strongly polar cation-coordinating solvent, and Li^+ coordination to diethyl ether moderates the Li^+ Lewis acidity.[35,36] Versus diethyl ether, nitromethane is moderately cation-coordinating as reflected in its donor number (19.2 versus 2.7 for diethylether and nitromethane, respectively).[23] Due to its higher dielectric constant and dipole moment, nitromethane enhances Li^+ Lewis acidity, and thus carbonyl group activation is more effective.[34–36]

We find in this work that acylations in the presence of $LiClO_4$ are accompanied by more rapid acetic acid formation, the concentration of which always equals that of the benzophenone formed. That the presence of $LiClO_4$ may increase Ln^{3+} Lewis acidity was probed by conducting the aforementioned $Gd(OTf)_3$−acetic anhydride line-broadening experiments in the presence of added $LiClO_4$ (see Figure 5). The NMR spectra are indistinguishable from these in the other $Gd(OTf)_3$−acetic anhydride coordination probing experiments, suggesting the effects on ground-state substrate coordination equilibria are small. While the exact role of $LiClO_4$ in $Ln(OTf)_3$-mediated FC acylation is not completely clear at this stage, it is conceivable that $LiClO_4$ + $Yb(OTf)_3$ anion metathesis[14e,g,25a] may facilitate highly reactive oxocarbenium perchlorate formation, $CH_3CO^+ClO_4^-$ (Figure 10, **I**). A similar mechanism was proposed for $SbCl_5$−$LiClO_4$- mediated FC acylation.[25a]

(30) Classical FC Lewis acidity effects: Brown, H. C.; Jensen, F. R. *J. Am. Chem. Soc.* **1958**, *80*, 2296–2300.

(31) (a) Hong, S.; Kawaoka, A.; Marks, T. J. *J. Am. Chem. Soc.* **2003**, *125*, 15878–15892. (b) Ryu, J. S.; Li, G. Y.; Marks, T. J. *J. Am. Chem. Soc.* **2003**, *125*, 12584–12605. (c) Hong, S.; Tian, S.; Metz, M. V.; Marks, T. J. *J. Am. Chem. Soc.* **2003**, *125*, 14768–14783.

(32) (a) Giardello, M. A.; Conticello, V. P.; Brard, L.; Gagné, M. R.; Stern, C. L.; Marks, T. J. *J. Am. Chem. Soc.* **1994**, *116*, 10241–10254. (b) Gagné, M. R.; Stern, C. L.; Marks, T. J. *J. Am. Chem. Soc.* **1992**, *114*, 275–294. (c) Jeske, G.; Schock, L. E.; Mauermann, H.; Swepston, P. N.; Schumann, H.; Marks, T. J. *J. Am. Chem. Soc.* **1985**, *107*, 8103–8110.

(33) (a) Acetic anhydride in classic FC acylation: Jeffery, E. A.; Satchell, D. P. N. *J. Chem. Soc.* **1962**, 1877–1894. (b) Satchell, D. P. N. *J. Chem. Soc.* **1960**, 1752–1768. (c) Van Dyke, R. E.; Crawford, H. E. *J. Am. Chem. Soc.* **1951**, *73*, 2018–2021. (d) Van Dyke, R. E. *J. Am. Chem. Soc.* **1951**, *73*, 398–402.

(34) Arene substituent effects in classical FC acylations: (a) Tashiro, M.; Kobayashi, S.; Olah, G. A. *J. Am. Chem. Soc.* **1970**, *92*, 6369–6371. (b) Tuzun, C.; Ogliaruso, M.; Becker, E. I. *Org. Synth.* **1961**, *41*, 1–4. (c) Marino, G.; Brown, H. C. *J. Am. Chem. Soc.* **1959**, *81*, 5475–5481. (d) Cullinane, N. M.; Chard, S. J.; Leyshon, D. M. *J. Chem. Soc.* **1952**, 376–380. (e) Cutler, R. A.; Stenger, R. J.; Suter, C. M. *J. Am. Chem. Soc.* **1952**, *74*, 5475–5481. (f) Shah, R. C.; Chaubal, J. S. *J. Chem. Soc.* **1932**, 650–652.

(35) (a) Springer, G.; Elam, C.; Edwards, A.; Bowe, C.; Boyles, D.; Bartmess, J.; Chandler, M.; West, K.; Williams, J.; Green, J.; Pagni, R. M.; Kabalka, G. W. *J. Org. Chem.* **1999**, *64*, 2202–2210. (b) Pagni, R. M.; Kabalka, W.; Bains, S.; Plesco, M.; Wilson, J.; Bartmess, J. *J. Org. Chem.* **1993**, *58*, 3130–3133.

(36) (a) Sudha, R.; Sankararaman, S. *J. Chem. Soc., Perkin Trans. 1* **1999**, 383–386. (b) RajanBabu, T. V. *J. Org. Chem.* **1984**, *49*, 2083–2088.

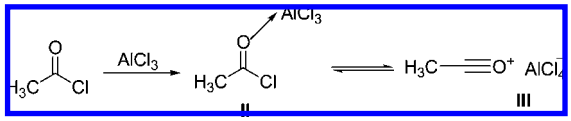

FIGURE 11. Electrophilic species generated from acyl halides and aluminum halides. **II**, donor−aceptor complex; **III**, acylium aluminate ion pair.

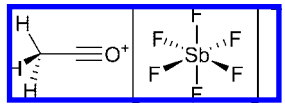

FIGURE 12. Perspective drawing of the methyloxocarbonium hexafluoroantimonate salt, $[CH_3CO]^+[SbF_6]^-$. Bond lengths: Sb−F = 1.894 Å (weighted average); C−C = 1.385 (16) Å; C−O = 1.108 (15) Å.[26]

Ln^{3+}−Substrate Interactions and the Nature of the Active Species. The activation process for acylation reactions involving Lewis acids depends on the identity of the acylating agent.[3,4] In classical Fridel−Crafts acylations with acid chlorides, it is known that their complexes with Lewis acids involve electrophilic intermediates, which exist in solution as either covalent (Figure 11, **II**)[25] or ion paired forms (Figure 11, **III**),[26] with the equilibrium position depending both on the nature of the acylating agent, the aromatic, solvent, and temperature.[3,30] Evidence for formation of 1:1 or 1:2 donor–acceptor covalent complexes (Figure 11, **II**), such as acetyl chloride−aluminum halide complexes in SO_2 solution, is provided by NMR spectroscopy.[25] Moreover, a number of stable crystalline acylium salts, such as methyloxocarbonium hexafluoroantimonate (Figure 12), have been characterized by X-ray diffraction, as well as solid state NMR and IR spectroscopy.[26]

In classical FC acylations, kinetic and mechanistic investigations along with conductivity measurements suggest that in reaction with aluminum halides, acetic anhydride behaves as an acyl halide−aluminum halide complex which effects the actual acylation (eqs 11 and 12).[33] Acetic anhydride reacts with 2 equiv of $AlCl_3$ to afford 2 equiv of acyl halide acylating agent.[33]

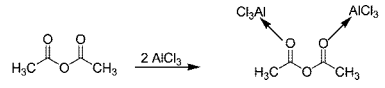

(11)

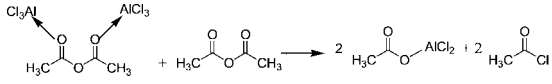

(12)

Describing Ln^{3+}−acetic anhydride interactions relies on understanding Ln^{3+} coordination chemistry.[7a–d,37c,d] While numerous lanthanide β-diketonates have been isolated and characterized crystallographically,[38] Ln^{3+}−β-diketone complexes have not been isolated, presumably due to their low

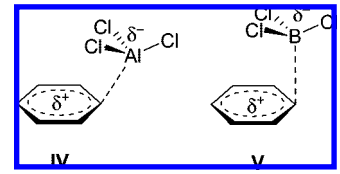

FIGURE 13. Ab initio results on geometry-optimized complexes **IV** (C_6H_6−$AlCl_3$) and **V** (C_6H_6−BCl_3).[40] In the monomeric state, $AlCl_3$ and BCl_3 possess D_{3h} geometries. However, in the complexed state, charge transfer from the benzene HOMO to Al^{3+} or B^{3+} leads to geometric distortion and pyramidalized complexes **IV** and **V**. This entails partial loss of benzene aromaticity, compensated to an extent by back-donation of Cl 3p electron density to the benzene HOMO. In complex **IV**, the greater charge on Al leads to a closer approach to the aromatic carbon (Al−C ≈ 2.35 Å), thus to more effective charge transfer than in complex **V**, with a longer computed B−C distance (≈ 3.22 Å).[40]

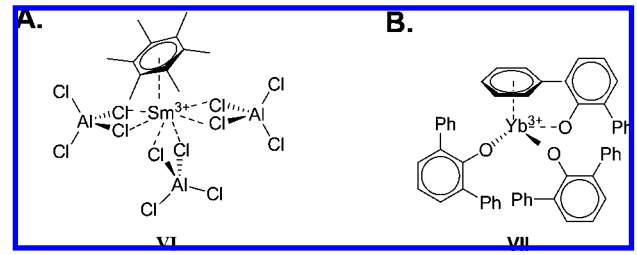

FIGURE 14. (A) Perspective drawing of the crystal structure of the arene complex $Sm(C_6Me_6)(AlCl_4)_3$, **VI**. (B) Perspective drawing of the crystal structure of the aryloxide complex $[Yb(O\text{-}2,6\text{-}Ph_2C_6H_3)_3]$, **VII**.

binding energies. However, Ln^{3+}−ketone complexes have been detected in solution by ^{13}C and ^{17}O NMR.[39]

In all proposed conventional FC acylation reaction mechanisms, the role of the Lewis acid, such as $AlCl_3$, is limited to generation of the electrophile, which subsequently attacks the arene to form either a π- or σ-complex (see Discussion section). Ab initio calculations have probed an additional role of the Lewis acid in C_6H_6−$AlCl_3$ and C_6H_6−BCl_3 model structures and indicate the marked tendency of only one arene carbon atom to become highly nucleophilic, thereby facilitating an attack by an incipient electrophile (Figure 13).[40]

In conjuction with the aforementioned ab initio studies, experimental work has shown that arenes form isolable π-complexes with electrophiles such as Sm^{3+}[16] and Ag^+.[17] Schwotzer and Cotton demonstrated that neutral arenes form isolable π-complexes with Sm^{3+} in a sterically congested mononuclear η^6-complex (Figure 14, **VI**).[16e,f] The Nd^{3+}, Gd^{3+}, and Yb^{3+} derivatives have been characterized and described as well.[16a] Later, it was shown that less-substituted arenes, such as *m*-xylene[16c] or even benzene, also yield isolable analogues of the type $Ln(C_6H_6)(AlCl_4)_3$ (Ln = La, Nd, Sm).[16d] A homoleptic Yb(III) aryloxide complex $[Yb(O\text{-}2,6\text{-}Ph_2C_6H_3)_3]$ was also shown to exhibit an intramolecular Yb^{3+}−π-arene interaction (Figure 14, **VII**).[16b] The existence of thermally stable

(37) (a) Gamp, E.; Shimomoto, R.; Edelstein, N.; McGarvey, B. R. *Inorg. Chem.* **1987**, *26*, 2177–2782. (b) Bertini, I.; Luchinat, C. *NMR of Paramagnetic Molecules in Biological Systems*; Benjamin: Menlo Park, 1986; Chapter 10. (c) Fischer, R. D. *Fundamental and Technological Aspects of Organo-f-Element Chemistry;* Marks, T. J., Fragalla, I. L., Eds.; Reidel Publishing: Dordrecht, 1985; Chapter 8. (d) McGarvey, B. R. *Organometallics of the f-Elements;* Marks, T. J., Fischer, R. D., Eds.; Reidel Publishing: Dordrecht, 1979; Chapter 10. (e) McGarvey, B. R. *Can. J. Chem.* **1984**, *62*, 1349–1355. (f) McGarvey, B. R. *J. Chem. Phys.* **1976**, *65*, 955–961. (g) Kolb, J. R.; Marks, T. J. *J. Am. Chem. Soc.* **1975**, *97*, 27–35. (j) Horrocks, W. D., Jr. *NMR of Paramagnetic Molecules;* La Mar, G. N., Horrocks, W. D., Holm, R. H., Eds.; Academic Press: New York, 1973; Chapter 4.

(38) Ln^{3+}−β-diketonates complexes: (a) Melby, L. R.; Rose, N. J.; Abramson, E.; Caris, J. C. *J. Am. Chem. Soc.* **1964**, *86*, 5117–5125. (b) Halverson, F.; Brinen, J. S.; Leto, J. R. *J. Chem. Phys.* **1964**, *40*, 2790–2792. (c) Whan, R. E.; Crosby, G. A. *J. Mol. Spectrosc.* **1962**, *3*, 315–327. (d) Pope, G. W.; Steinbach, J. F.; Wagner, W. F. J. *Inorg. Nucl. Chem.* **1961**, *20*, 304–313. (e) Biltz, W. *Justus Lieb. Ann. Chem.* **1904**, *331*, 334–358.

(39) (a) Raber, D. J. *J. Chem. Soc., Perkin Trans. 2* **1986**, 853−859. (b) Okuyama, T.; Fueno, T. *J. Am. Chem. Soc.* **1980**, *102*, 6591–6594. (c) Chadwick, D. J.; Williams, D. H. *J. Chem. Soc., Perkin Trans. 2* **1974**, 1202−1206.

(40) $AlCl_3$−and BF_3−arene ab initio calculations: Tarakeshwar, P.; Lee, J-Y.; Kim, K. S. *J. Phys. Chem. A* **1998**, *102*, 2253–2255.

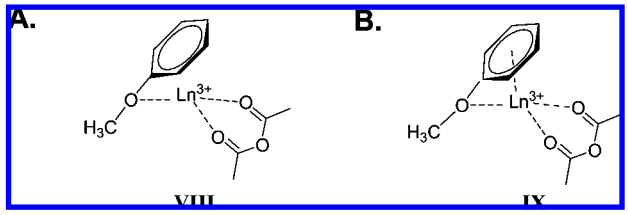

FIGURE 15. (A) Anisole coordination to Ln^{3+} through the methoxy oxygen only, **VIII**. (B) Anisole coordination to Ln^{3+} through the methoxy oxygen and arene π-complexation, **IX**.

Ln^{3+}−arene complexes provides precedent for Ln^{3+}−arene complexation in the present catalytic arene acylations. In principle, anisole coordination to Ln^{3+} could occur through the methoxy oxygen only (Figure 15, **VIII**) or accompanied by additional arene π-cloud Ln^{3+} polarization (Figure 15, **IX**).

As discussed above, acetic anhydride−Ln^{3+} complexation was probed by ^{1}H NMR spectroscopy using the coordinatively unsaturated, $4f^7$ paramagnetic NMR broadening probe, $Gd(OTf)_3$. Gd^{3+} complexes, by virtue of their ground state ($^8S_{7/2}$, $<S_Z>_J \approx -31.5$),[37] are magnetically isotropic and cannot give rise to dipolar (or pseudocontact) shifts but can give rise to contact shifts.[37] Because of the slow electronic spin–lattice relaxation in Gd^{3+}, NMR spectra of these complexes are usually very broad, as also observed in this study (Figure 5). Incremental addition of $Gd(OTf)_3$ to acetic anhydride solutions in nitromethane causes slight downfield displacement (versus internal 1,1,2,2,-tetrachloroethane) of the acetic anhydride methyl resonance from δ 2.094 ppm to δ 2.243 ppm (see Results Section above on Coordination Probing, Figure 5) and far greater line-broadening of the acetic anhydride resonance than that of the nitromethane peak. This behavior can be interpreted in terms of equilibria as in eq 13, where ligand exchange is rapid on the NMR time scale at room temperature. Also, the small observed downfield paramagnetic shift is consistent with minor ligand

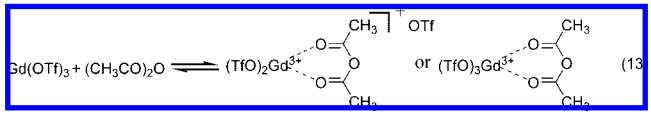

electron density donation (π-electrons from carbonyl) into (or polarization by) empty or partially filled Gd^{3+} orbitals (4f or 6s, 6p, 5d in the present case) with exchange interactions favoring transfer of spin density parallel to the spin already on Gd(III), leaving unpaired spin density of the opposite sign remaining on the ligand.[6,25,26,32] The effect should attenuate as the number of bonds between metal and the interacting nucleus is increased, hence the small change in the methyl ^{1}H chemical shift.

Both structures proposed in eq 13 depict acetic anhydride binding to Ln^{3+}. The NMR data suggest that, in nitromethane, formation of a Lewis acid–base complex between acetic anhydride and the Ln^{3+} center occurs. Note that while lanthanide triflates are poorly soluble in nitromethane, addition of acetic anhydride immediately induces dissolution. These observations along with the aforementioned NMR shifting/line-broadening results support the suggestion that initial activation of acetic anhydride by $Ln(OTf)_3$ precatalyst leads to the formation of the active catalyst (Figure 16).

The viability and the type of Ln^{3+}−arene complexation suggested in Figure 15 was also investigated spectroscopically utilizing coordinatively unsaturated paramagnetic NMR probes (Gd^{3+}, Yb^{3+}) on both individual and competitive levels. The former involved incremental $Gd(OTf)_3$ addition to a nitromethane solution of anisole at constant [anisole] (see Results above on Coordination Probing). The results are inconclusive due to extensive line-broadening of all the anisole peaks and merging of the methoxy and nitromethane resonances, even with $Gd(OTf)_3$:anisole = 0.1:1. However, competition studies reveal more information (Figure 6). Incremental addition of $Gd(OTf)_3$ to the reaction mixture of anisole and acetic anhydride in nitromethane solution induces line-broadening of both arene aromatic and acetic anhydride resonances, with slightly greater broadening of the latter (for line width at half-height ratios, see Figure 6), thus providing evidence for the latter type of Ln^{3+}−subtrate interaction proposed in structure **IX**, Figure 15.

For $Yb(OTf)_3$, unlike $Gd(OTf)_3$, strong spin–orbit coupling results in a rapid electron spin–lattice relaxation, resulting in a reasonable NMR sharp line widths and expectation of substantial dipolar shifts.[19,37] Analysis of $Yb(OTf)_3$-mediated anisole acylation with acetic anhydride in nitromethane-d_3 solutions reveals a slight downfield displacement of the methoxy peak ($\Delta \sim 0.06$ ppm) vs the 1,1,2,2-tetrachloroethane internal standard, suggesting weak coordinative interactions between the methoxy oxygen and Yb^{3+}, supporting proposed structure **VIII** in Figure 15. Furthermore, the aromatic proton chemical shift dispersion in $Yb(OTf)_3$-mediated thioanisole and anisole acylation (Figure 7) increases markedly on $Yb(OTf)_3$ addition, providing evidence for Yb^{3+}−arene complexation as well (e.g., **IX** in Figure 15).

Mechanism of Catalytic $Ln(OTf)_3$-Mediated Acylation. As noted above, the present kinetic results for $Ln(OTf)_3$-catalyzed anisole acetylation with acetic anhydride indicate first-order rate dependence on both substrate and catalyst concentrations. Earlier kinetic and mechanistic studies of classical FC acylation suggested that acetic anhydride behaves as an acyl halide and that in polar solvents such as nitromethane, heterolysis favors an acylium ion (CH_3CO^+) pathway, because of greater transition state stabilization/solvation in polar solvents.[21,26] However, the acylium is a relatively weak electrophile,[3] and acylation of even slightly deactivated aromatics is sluggish.[3,4]

The proposed $Yb(OTf)_3$-catalyzed reaction mechanism (Figure 16) has several steps: (i) activation of acetic anhydride via $Ln(OTf)_3$ coordination, (ii) formation of an anisole complex. The arene aromaticity is not yet lost in the substrate−reagent complex. As the reagents move closer to bonding distance, (iii) anhydride C−O bond heterolysis occurs, possibly facilitated by arene π-complex formation, to generate a reactive electrophile CH_3CO^+, along with (iv) aromatic deprotonation with benzophenone and acetic acid generation. Kinetic isotope data suggest the deprotonation step to be the turnover-limiting step.

That the results of this anaerobic/anhydrous study (e.g., Ln^{3+} effect on percent yield) parallel those reported by Kobayashi[11b] suggests that under less rigorous reaction conditions water ligands surrounding the Ln^{3+} center rapidly exchange with substrate, allowing their coordination to the Ln^{3+} center and the reaction to proceed. Furthermore, neutral Ln^{3+}−η^6-arene complexes synthesized under aerobic/hydrous Friedel–Crafts reaction conditions are isolable.[16] Thus for all aforementioned reasons, and under less anaerobic/anhydrous reaction conditions, it is likely that the proposed catalytic pathway in Figure 16 will most likely be unchanged.

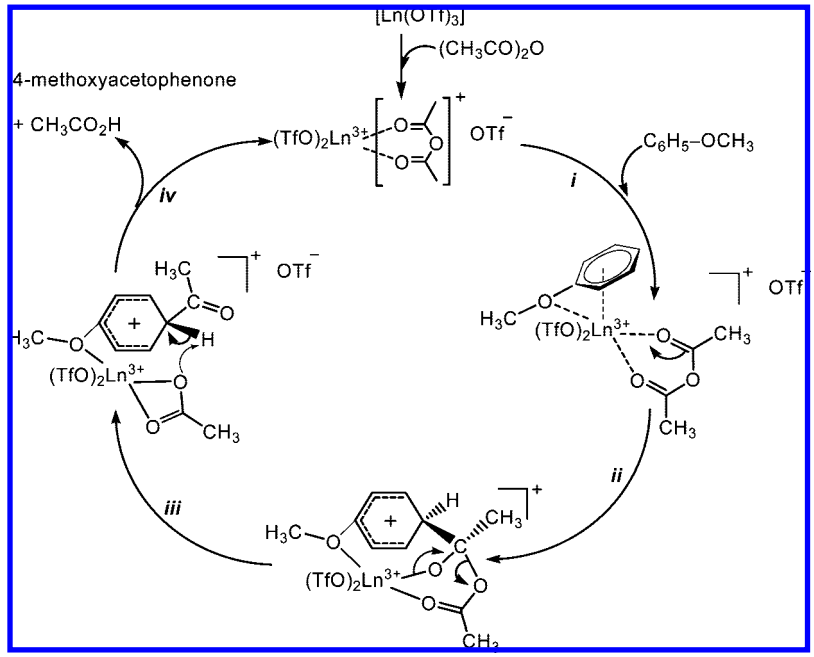

FIGURE 16. Mechanistic scenario for $Ln(OTf)_3$-mediated acylation of anisole with acetic anhydride in nitromethane.

Conclusions

Lanthanide triflates are clearly more efficient and cleaner arene acylation catalysts than conventional Lewis acids. They offer distinctive advantages such as the catalytic stoichiometry of $Ln(OTf)_3$ required to mediate FC acylations. Moreover, their air- and moisture-stability and efficient catalyst recyclability add an environmentally friendly aspect to $Ln(OTf)_3$ catalysis.

The mechanistic results presented here, which focus on the catalyst role, demonstrate that the present catalytic reaction pathway has similarities to, and differences from, more classical Lewis acid acylation. The first step in the classical FC acylation pathway consists of initial Lewis acid activation of the acylating agent. In classical FC acylation, acetic anhydride reacts with 2 equiv of Lewis acid to afford 2 equiv of acyl halide, which through Lewis acid-coordination/abstraction generates the reactive electrophile, CH_3CO^+, which effects the actual acylation. The sequence of events leading to reactive electrophile generation using $Ln(OTf)_3$ appears to be markedly different. Acetic anhydride activation via $Ln(OTf)_3$ coordination is followed by Ln^{3+}−arene π-complex formation, which possibly facilitates anhydride C−O bond heterolysis to generate the reactive electrophile. The last step, common in both pathways, is aromatic C−H bond scission with concurrent benzophenone generation. Both classical FC and the kinetic isotope data presented herein suggest C−H scission to be turnover-limiting.

In addition to mechanistic pathway differences, other notable differences/similarities for classical FC versus $Ln(OTf)_3$-mediated acylation include Lewis acidity effects on the overall reaction order, arene substituent effects, and solvent effects. In classical FC acylation, the overall reaction order is Lewis acidity-dependent, being higher order with weaker Lewis acids. However, in $Ln(OTf)_3$-mediated acylation, the reaction order for different Ln^{3+} ions is unchanged, suggesting minimal ionic radius-dependent steric constraints in the transition state. While classical Lewis acids effectively catalyze acylation of activated and unactivated arenes, $Ln(OTf)_3$ efficiency is limited to activated ones. Also, classical Lewis acids function in both polar and nonpolar solvents while the effectiveness of $Ln(OTf)_3$ catalysts is limited to polar aprotic, moderately coordinating solvents such as nitromethane. Given these differences, acylations using $Ln(OTf)_3$ offer many attractions over classical Lewis acids: the acylations are catalytic, and the air- and moisture-stable catalysts can be recycled many times.

Experimental Section

Materials and Methods. All manipulations of reagents were carried out with rigorous exclusion of oxygen and moisture in flame- or oven-dried Schlenk-type glassware on a dual-manifold Schlenk-line, or interfaced to a high-vacuum line (10^{-6} Torr), or in a nitrogen-filled MBraun glovebox with a high-capacity recirculator (<1 ppm O_2). Argon (prepurified) was purified by passage through a MnO oxygen-removal column and a Davison 4-Å molecular sieve column. Nitromethane-d_3, used for NMR-scale reactions, was freshly predistilled under reduced pressure, dried over $CaCl_2$, and stored over activated Davison 4-Å molecular sieves in a vacuum-tight storage flask under an Ar atmosphere. All aromatic substrates, unless stated otherwise, were purchased from a chemical supplier, distilled under reduced pressure, and dried as appropriate prior to use. Acetic anhydride was predistilled and dried over BaO in a vacuum-tight storage flask under an Ar atmosphere prior to use.

Physical and Analytical Measurments. Solution NMR spectra were recorded either on a Varian Inova-500 (FT, 500 MHz, ^{1}H) or Varian Inova-400 (FT, 400 MHz, ^{1}H) NMR spectrometer equipped with a variable-temperature unit. All ^{1}H NMR chemical shifts are reported relative to 1,1,2,2-tetrachloroethane, an internal reference standard, unless stated otherwise. Thermogravimetric (TGA) and differential thermal analysis (DTA) data were collected on a TA Instruments model SDT 2960 at atmospheric pressure, with an N_2 flow rate of 100 mL/min and a temperature ramp of 5 °C/min. X-ray diffraction (XRD) data were acquired with a computer-interfaced Rigaku DMAX-A powder diffractometer using Ni-filtered Cu Kα radiation.

Preparation of $Ln(OTf)_3$ Complexes. All lanthanide triflate salts (Ln = La, Sm, Eu, Gd, Yb, Lu) were prepared by adding an excess of respective lanthanide(III) oxide (99.9% purity) to an aqueous solution of trifluoromethanesulfonic acid (50% v/v) and heating at boiling for approximately 1 h.[41a] The mixture was then filtered to remove the unreacted oxide, and the water was then removed from the filtrate under reduced pressure. The resulting hydrate was further

dried by heating under a vacuum at 180−200 °C for 48 h. The resulting anhydrous $Ln(OTf)_3$ complexes were stored in a glovebox under a nitrogen atmosphere. Formation of the desired products was confirmed by TGA, DTA, and XRD.[41]

Preparation of Standard Solutions for Kinetic Studies. For each data set, a separate standard solution was prepared under inert atmosphere in a three-neck round-bottom flask interfaced to a high-vacuum line. The solution consisted of nitromethane-d_3, an internal NMR standard, and either the aromatic substrate or acylating agent, whichever was to be held in pseudofirst-order excess, depending on the particular kinetic experiment.[42]

Typical NMR-Scale Catalytic Reaction. In the glovebox, a J-Young NMR tube equipped with a Teflon valve was loaded with a precatalyst $Ln(OTf)_3$ (Ln = La, Eu, Yb, Lu), except for the studies in which $LiClO_4$ cocatalyst effects were explored, in which the cocatalyst loading with respect to the catalyst was 6-fold. On the high-vacuum line, the tube was evacuated (10^{-6} Torr), then frozen at −78 °C, followed by addition of 700 μL of the standard solution and the second substrate via gastight syringe to the NMR tube under an argon flush. The tube was then evacuated and backfilled with Ar while frozen at −78 °C and then sealed with the Teflon valve. The frozen reaction mixture was maintained in a dry ice/acetone bath until the beginning of the kinetic run.

Kinetic Studies of $Yb(OTf)_3$-Mediated Acylation. In a typical NMR experiment, an NMR sample was prepared as described above (see Typical NMR-Scale Catalytic Reaction section) but maintained at −78 °C until kinetic measurements were begun. The sample tube was then inserted into the probe of the NMR spectrometer, which had been previously set to the appropriate reaction temperature ($T \pm 0.2$ °C, calibrated with the ethylene glycol temperature standard). A long pulse delay was used during data acquisition to avoid saturation. All data for a particular set of kinetic runs were collected using a single preacquisition delay, which was adjusted to fit the overall reaction times. The kinetics were usually monitored from intensity changes in the substrate alkoxy or acetic anhydride methyl resonances over three or more half-lives.

The substrate concentration C as a function of time was calculated with respect to the known concentration of a 1,1,2,2-tetrachloroethane standard in the solution. The turnover frequency (h^{-1}; eq 14) was calculated from the least-squares-determined × intercept ($-C_0/m$, min) where C_0 is the initial substrate concentration and E is the catalyst to substrate ratio.[31,42]

$$N_t(h^{-1}) = (60 \text{ min } h^{-1}/(-C_0/m))E \qquad (14)$$

Activation Parameters and Associated Errors. Eyring and Arrhenius kinetic analyses[20] of data obtained in variable-temperature experiments were used to extract $\Delta H^{\ddagger}$, $\Delta S^{\ddagger}$, and E_a parameters. The errors in these activation parameters were computed from the published error propagation formulas (eqs 15 and 16)[20a] which were derived from the Eyring equation[20b] using the OriginPro 7.5 program.

Absolute Error in $\Delta H^{\ddagger}$:

$$(\sigma\Delta H^{\neq})^2 = \frac{R^2T_{max}^2T_{min}^2}{\Delta T^2}\left\{\left(\frac{\sigma T}{T}\right)^2\left[\left(1+T_{min}\frac{\Delta L}{\Delta T}\right)^2 + \left(1+T_{max}\frac{\Delta L}{\Delta T}\right)^2\right] + 2\left(\frac{\sigma k}{k}\right)^2\right\} \qquad (15)$$

Absolute Error in $\Delta S^{\ddagger}$:

$$(\sigma\Delta S^{\neq})^2 = \frac{R^2}{\Delta T^2}\left\{\left(\frac{\sigma T}{T}\right)^2\left[T_{max}^2\left(1+T_{min}\frac{\Delta L}{\Delta T}\right)^2 + T_{min}^2\left(1+T_{max}\frac{\Delta L}{\Delta T}\right)^2\right] + \left(\frac{\sigma k}{k}\right)^2(T_{max}^2+T_{min}^2)\right\} \qquad (16)$$

Isotopic Labeling Studies. The substrate [4-^{2}H]anisole was synthesized by treat 4-bromoanisole with Mg turnings to form the corresponding Grignard reagent, (*p*-methoxyphenyl)magnesium bromide, which was quenched with D_2O. The final product was first extracted with ether, then fractionally distilled under reduced pressure, and finally stored in a closed storage vessel under nitrogen.[43] Characterization by ^{1}H NMR 500 MHz CD_3NO_2: δ 3.796 (s, 3H, OMe), 6.935 (d, J = 7.9 Hz, 2H), 7.304 (d, J = 7.9 Hz, 2H).

Paramagnetic Line-Broadening Experiments on Individual Substrates. In the glovebox, a J-Young NMR tube equipped with a Teflon valve was loaded with various quantities of the paramagnetic ($4f^7$) $Gd(OTf)_3$ precatalyst. On the high-vacuum line, each tube was evacuated to 10^{-6} Torr, then frozen at −78 °C. Under an argon flush of 600 μL of the nitromethane-d_3 standard solution, consisting of 6.36 M acetic anhydride or 6.36 M acetic anhydride with 0.41 M $LiClO_4$ or 6.36 M anisole, 0.05 M 1,1,2,2-tetrachloroethane was added via gastight syringe into each NMR tube, which was then sealed with the Teflon valve. The NMR tubes were then evacuated and backfilled with argon. ^{1}H NMR spectra were recorded at room temperature, and resonance line width at half-height ratios were obtained from individual peak measurements. Gd^{3+}-induced line broadening of the anisole spectrum causes partial merging of the methoxy and nitromethane resonances as well as of the two aromatic resonances.

Paramagnetic Line-Broadening Experiments on Reaction Mixtures. In the glovebox, J-Young NMR tubes equipped with a Teflon valve were loaded with varying amounts of the paramagnetic ($4f^7$) $Gd(OTf)_3$ precatalyst. On the high-vacuum line, each tube was evacuated to 10^{-6} Torr, then frozen at −78 °C. Under an argon flush, of 600 μL of the nitromethane-d_3 standard solution, consisting of 0.917 M acetic anhydride and 0.132 M anisole, 0.263 M 1,1,2,2,tetrachloroethane was added via gastight syringe into each NMR tube, which were then sealed with the Teflon valve. The NMR tubes were then evacuated and backfilled with argon. ^{1}H NMR spectra were recorded at room temperature, and resonance line width at half-height ratios were obtained from individual peak measurements.

Acknowledgment. We gratefully acknowledge financial support by NSF (CHE-04157407). We also thank Dr. X. Yu for helpful suggestions on the kinetic studies.

JO800158K

(41) $Ln(OTf)_3$ preparation and characterization: (a) Pascal, J. L.; Hamidi, M. M. *Polyhedron* **1994**, *11*, 1787–1792. (b) Abbasi, A.; Lindqvist-Reis, P.; Eriksson, L.; Sandstrom, D.; Lidin, S.; Persson, I.; Sandstrom, M. *Chem.−Eur. J.* **2005**, *11*, 4065–4077. (c) Egashira, K.; Yoshimura, Y.; Kanno, H.; Suzuki, Y. *J. Therm. Anal. Calorim.* **2003**, *71*, 501–508. (d) Zineddine, H.; Hnach, M.; Hamidi, M. *J. Fluorine Chem.* **1998**, *88*, 139–141. (e) Nakayama, M.; Nakamura, S.; Yanagihara, N. *Polyhedron* **1998**, *17*, 3625–3631.

(42) (a) *Investigation of Rates and Mechanism of Reactions*; Bernasconi, C., Ed.; 4th ed.; Interscience: New York, 1986. (b) BensonS. W. *Thermochemical Kinetics*, 2nd ed.; Wiley & Sons: New York, 1986; pp 8−10.

(43) Abdul-Malik, N. F.; Jenkins, L. A.; Davis, F. A. *J. Org. Chem.* **1983**, *48*, 5128–5130.